High-Field Franz-Keldysh Effect and Exciton Ionization in Semiconductor Quantum Wires

S. Hughes
Department of Physics, University of Surrey, Guildford, Surrey GU2 5XH, United Kingdom

D. S. Citrin
Department of Physics, Washington State University, Pullman, Washington 99164-2814
(Received 11 October 1999)

We investigate the Franz-Keldysh effect and exciton ionization in semiconductor quantum wires. Absorption spectra are calculated near the band gap by solution of the low-density semiconductor Bloch equations in real space. The Sommerfeld factor and field-induced tunnel ionization of the exciton significantly affect the continuum portion of the absorption spectrum and remove the well known divergence problem associated with the 1D density of states at all field strengths. For reasonable electric field strengths substantial and tunable absorption oscillations appear above the band gap. Moreover, for very large fields, transparency can be achieved in the continuum for certain spectral positions.

PACS numbers: 78.47.+p, 42.50.Md, 71.35.–y

Semiconductor quantum wires offer a unique playground for investigating how electrons and holes move in one dimension [1]. A surprising feature of the 1D system is the inverse-square-root divergence of the joint density of states (DOS) at the band gap. However, as pointed out in Ref. [2], the Sommerfeld factor, which is the intensity ratio of the optical density associated with excitonic scattering states to the free electron-hole (e-h) pair above the band gap, removes this divergence. Moreover, in contrast to the 2D and 3D cases, the Sommerfeld factor is <1 for all frequencies above the band gap. Consequently, the singular 1D DOS does not show up at all in the linear absorption spectrum.

With regard to the Franz-Keldysh effect (FKE) in bulk crystals, the influence of a *strong* constant electric field $\mathbf{F}$ on the optical and electronic properties of semiconductors was brought to the fore over four decades ago [3]; no ground state of the e-h pair exists under the aforesaid conditions, and one must go beyond the usual Bloch-function picture. For 2D semiconductors, such as quantum wells [4], similar effects occur for a field polarized in the plane, while the quantum-confined Stark effect prevails for fields polarized in the growth direction. Electric-field effects for currents applied in the growth direction have also been studied for quantum-well wires (QWW's) [5]. However, to the best of our knowledge the FKE has not yet been investigated for semiconductor QWW's though Coulomb ionization effects have been and remain to be intensely investigated for 1D atomic systems [6]. Our motivation is also partly due to trends: Both experimental [7] and theoretical [8,9] studies on semiconductor QWW's are receiving renewed interest as a result of excellent strides in growth technology resulting in high quality samples with well defined characteristics. Additionally, from a theoretical viewpoint high-field effects in semiconductors are of interest to explore related phenomena in atomic systems, such as above threshold ionization and stabilization. These studies are also important for elucidating the fundamental physics of 1D semiconductors, a prerequisite, if you like, for device applications ranging from nanotechnology to semiconductor laser systems [10].

We study the FKE on QWW's by solving the semiconductors Bloch equations (SBE) in real space. The motivation behind the real-space approach is twofold: (i) as a probe into the e-h wave packet (WP) motion and (ii) to implement a very efficient fast Fourier transform algorithm. We begin our study in the spirit of nonperturbative quantum mechanics by employing an effective 1D Schrödinger equation (in excitonic units):

$$i\,\frac{\partial}{\partial t}\,\Psi(x,t) = \left[E_{\mathrm{g}} - \frac{\partial^2}{\partial x^2} - V(x) + xF\right]\Psi(x,t)\,, \quad (1)$$

where x is the relative distance between an electron and hole, $\Psi(x,t)$ is the quasi-one-dimensional WP, F is the electric field applied along the wire direction, and V is the Coulomb potential whose specific form is discussed below.

A fully quantum method for integrating numerically the above equation without using a restrictive basis expansion can be implemented by employing the split-step method [11,12]. The essence of this method is to carry out the action of the kinetic operator efficiently in Fourier space, while the action of the potential operator is carried out in real space. Absorbing boundary conditions can be implemented to remove any part of the wave packet reaching the boundaries, so that artificial reflections are avoided. As an initial approach, and as is often the starting point for related atomic studies, the ground state wave function can be obtained simply by imaginary time integration [11]. However, since we are interested in the optical properties, we thus need to consider the original source, i.e., an optical field, and hence we reformulate the wave packet equation in terms of the polarization,

$$i\,\frac{\partial}{\partial t}\,P_{ab}(x,t) = \left[E_{\mathrm{g}} - \frac{\partial^2}{\partial x^2} - V_{ab}^{ab}(x) + xF - i\Gamma\right] \times P_{ab}(x,t) + \Omega(t)\delta(x)\,, \quad (2)$$

 0031-9007/00/84(18)/4228(4)$15.00

where $\Omega(t) = d_{ab}\varepsilon(t)$ is the Rabi energy with d_{ab} the interband dipole moment and $\varepsilon(t)$ the optical pulse, Γ^{-1} is the dephasing time, and P_{ab} is the induced polarization between two subbands a and b. We assume that the optical pulse is excited resonantly with the band gap and hence the detuning does not appear explicitly. For the time being we concentrate on a two-subband semiconductor model ($ab = 1e - 1hh$) but will later discuss the role of multisubbands as well as Coulomb mixing effects. As convenient in the absence of a more specific model for the QWW potential we will assume that the electrons and holes are confined laterally by a harmonic oscillator potential with a subband spacing of $\Omega_{j=e,h}$. Moreover, we assume perfect confinement in the growth direction. The Coulomb interaction between charge carriers thus becomes (again we use excitonic units) $V_{ab}^{ab}(x) = 2\int dy \int dy' \frac{\psi_a(y)\psi_b^*(y')\psi_a(y)\psi_b^*(y')}{\sqrt{x^2+(y-y')^2}}$, where $\psi_j(y)$ are the eigenfunctions [9] associated with the lateral carrier motion, $\psi_n^{j=e,h}(y) = (\frac{1}{2^n n!}\sqrt{\frac{\mu\Omega_j}{m_j 2\pi}})^{\frac{1}{2}} \exp[-(\mu\Omega_j/m_j)y^2]H_n(\sqrt{\frac{\mu\Omega_j}{2m_j}}\, y)$, with μ the reduced mass, m_j the mass of an electron or hole, and H_n the Hermite polynomial. The Fourier transform of Eq. (2) is exactly equivalent to the SBE in the low-density limit [13,14]. The real-space approach is, however, a more natural choice here since we are interested in the effects of a strong electric field and its influence of the e-h spatial WP motion.

We employ material parameters typical of GaAs with a bulk exciton binding energy $E_0 = 4.2$ meV and Bohr radius $a_0 = 140$ Å. For the eigenfunction calculations we choose subband spacings of $3E_0$ for the holes and $7E_0$ for the electrons, and $m_h = 5m_e$. This results in holes that are more strongly confined than the electrons which is typical of real QWW's. The relevent observable in a usual experiment is the absorption coefficient $\alpha(\omega) \propto \mathrm{Im}[P(\omega)/|\varepsilon(\omega)|^2]$, where the polarization and electric field are slowly varying quantities. The optical polarization is simply $P(t) = d_{ab}P_{ab}(x = 0, t)$. For the electric field we choose a *weak* Gaussian pulse with a 40 fs full width at e^{-2} maximum irradiance. We choose a real-space region of $\pm 150a_0$ with 4096 discretized spatial points and numerically propagate with a time step of 0.1 fs. The computational technique is extremely efficient [15]. We first calculate an absorption spectrum with a dephasing time of 500 fs in the absence of an external field **F**. In Fig. 1(a) various snapshots of the polarization WP ($|P|^2$) are shown at the respective times: 0 fs (solid curve), 400 fs (dashed curve), and 600 fs (dotted curve); Fig. 1(b) shows the corresponding absorption spectrum. The time $t = 0$ fs coincides with the center of the optical pulse. We verify that the Coulomb interaction removes the singularity at the band gap associated with the 1D DOS [2,13]. The $1s$ binding energy is about 11 meV, 2–3 times the bulk value. We also show the absorption spectrum in the presence of 2-meV inhomogeneous broadening [16] (dashed line). For this calculation we carried out a standard convolution with a normalized Gaussian distribution after first obtaining the original absorption spectrum. To demonstrate the power of our technique we also calculate an absorption spectrum with a long dephasing time of 2 ps in the absence of an external field **F**, shown as an inset in Fig. 1(b); the $2s$ exciton is also clearly resolved though inhomogeneous broadening apparently destroys any signatures of this resonance. We mention that by using an SBE approach in k space the $2s$ exciton is very difficult to obtain because of numerical requirements at long dephasing times. The WP snapshots highlight the physics; shortly after the pulse arrives there is a strong probability for the electrons and holes to be Coulombically bound, hence the sharp peak near the center of the relative motion space. At later times the WP spreads and quantum beating occurs between the continuum states and the excitonic states. The WP ultimately speads out and dephases.

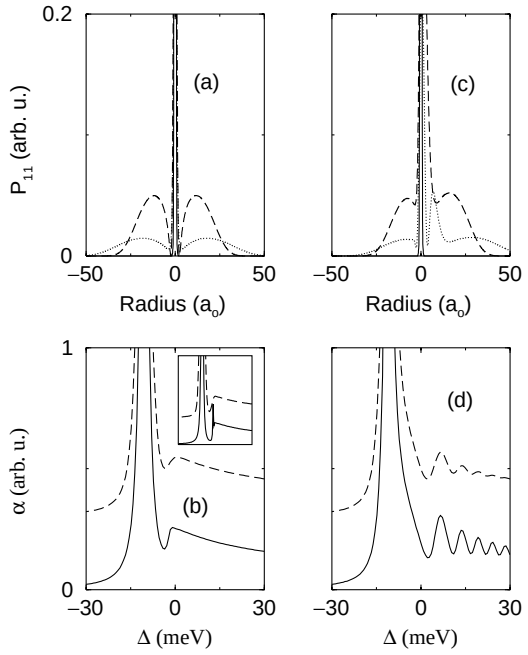

FIG. 1. (a) WP at several times (solid curve: $t = 0$ fs, dashed curve: $t = 400$ fs, and dotted curve: $t = 600$ fs). The spatial dimension is in units of the bulk exciton Bohr radius. The dephasing time is 500 fs. (b) Optical absorption spectrum versus detuning from the band gap without (solid line) and with inhomogeneous broadening (dotted line). The dotted curve has been shifted vertically for clarity. The inset shows identical calculations but with a dephasing time of 2 ps. (c) As in (a) but with a field energy (eFa_0) of $0.8E_0$. (d) As in (b) but with a peak field energy of $0.8E_0$.

Next we add an electric field aligned along the QWW axis (x direction). In Figs. 1(c) and 1(d) we display, respectively, WP snapshots and the resulting absorption spectrum for a field energy of $0.8E_0$ (corresponding field strength of 2.4 kV/cm). These energies are quoted in terms of eFa_0. In addition to a reduction of the $1s$

oscillator strength (of about 50%) and complete ionization of the $2s$ exciton, the free carrier-continuum portion of the spectrum exhibits pronounced oscillations that decrease in amplitude for higher energies. The WP is now strongly distorted, asymmetric, and propagates off to the right.

Now we employ very high fields and compare to the free carrier results, with energies greater than the quantum wire $1s$ binding energy. Specifically we adopt the field energy of $4E_0$ (12 kV/cm). In this regime, complete exciton ionization is expected. How do exciton effects modify the spectrum above the band gap since one expects signatures of a singularity for the free carrier results? Figure 2(a) shows snapshots of the WP at $t = 0$ fs and $t = 400$ fs; substantial interference effects are now evident for the propagating WP. In Fig. 2(b) is shown the corresponding absorption spectrum. Very large FK oscillations now occur even in the presence of inhomogeneous broadening. Figures 2(c) and 2(d) show identical calculations but without the Coulomb interaction; first a sharp discontinuity is not obtained as a result of field-induced tunneling although the spectrum does tend to rise more and more for frequencies approaching the band gap. The oscillations have a slightly different frequency separation and larger amplitude in the free carrier case since the Sommerfeld factor tends to inhibit the free excitons. The free carrier WP smoothly propages to the right, spreads, and dephases. Further numerical investigation [see the inset in Fig. 2(d)] at even higher fields results in a deeper modulation of the oscillations and an increase in the width of the oscillations. Moreover, field-induced transparency can be achieved at particular spectral positions; there is also a continuing shift of the free carrier spectrum to lower energies (not shown). We note that the tunability of the peaks and the deep modulations are unique for QWW's and cannot be obtained for 2D and 3D semiconductors because of their relatively large background absorption and lower tunneling rates. Indeed for quantum wells and bulk semiconductors the FK oscillations are typically rather small even for very large field strengths [13]. The reason for the present, substantial oscillations is because ionization tunneling in 1D systems is apparently much easier. Further, the results obtained with a dephasing time of 2 ps or in the limit of no background dephasing are almost identical to those above indicating that the broadening is primarily due to field-induced tunneling. The broadening can be understood as an uncertainty principle effect; soon after the excitons are created, they are destroyed by field ionization, and hence the energy resonance is broadened by lifetime broadening [4].

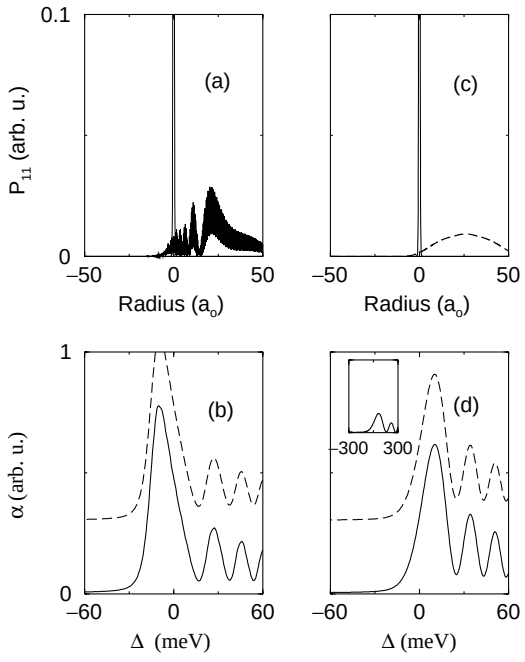

FIG. 2. (a) WP at several times (solid curve: $t = 0$ fs, and dashed curve: $t = 400$ fs. The background dephasing time is 500 fs and the peak field energy is $4E_0$. (b) Optical absorption spectrum (with and without inhomogeneous broadening). (c) As in (a) but without excitons. (d) As in (b) but without excitons; the inset shows the absorption spectra obtained for the higher field strength of $16E_0$. (The exciton case is almost indistinguishable.)

Finally we employ a multisubband model with one conduction subband ($1e$) and four valence subbands ($1hh$, $2hh$, $3hh$, $4hh$). Since we are dealing with symmetric wires for this study only two WP's contribute to the optical properties at low density: P_{11} and P_{13}. Consequently, we now have to solve two coupled polarization equations that are coupled through the Coulomb matrix elements, V_{ab}^{cb}, which now appear as a summation in the propagation equations for the polarization WP's. We stress that full Coulombic coupling is taken into account self-consistently by calculating the appropriate Coulomb and interband matrix elements. Figure 3(a) depicts the WP snapshots at $t = 0$ fs and $t = 400$ fs for both P_{11} and P_{13}; note that the scales are adjusted accordingly to account for the different dipole matrix elements. The corresponding absorption spectra [Fig. 3(b)] now exhibit two peaks separated by $6E_0$ (2 times the subband spacing). Figures 3(b) and 3(d) depict identical calculations with the field strength of $4E_0$, while Fig. 3(b) shows the corresponding WP's. Surprisingly the structure of the second allowed transition is completely washed out and the results are almost identical to those shown in Fig. 2(d). In relation to high-field transport experiments [17,18] effects such as transient velocity overshoot will not show up in our present study since we are dealing with the optical properties—where the only contributing spatial dynamics is at $x = 0$. Transport features and time-dependent field effects, i.e., the dynamic FKE [19], will be investigated at a later date.

In conclusion we have studied the FKE and exciton ionization on QQW's by solving the SBE in real space. Exciton ionization effects were highlighted by probing the electron-hole wave packet motion. For reasonable electric

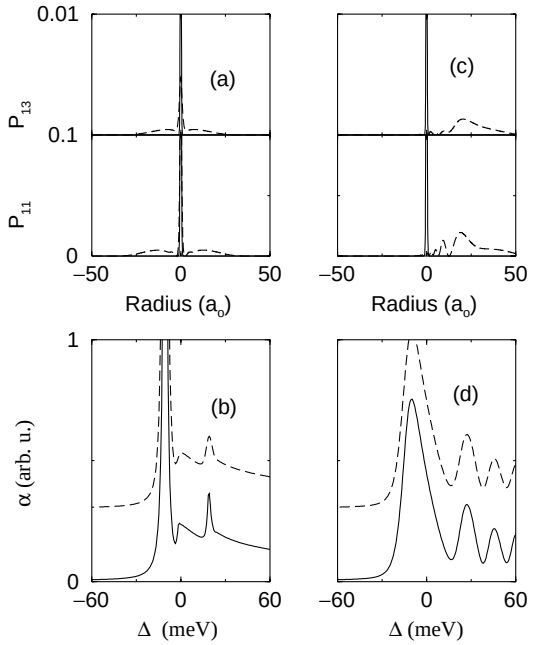

FIG. 3. Multisubband WP's P_{11} and P_{13} at several times (solid line: $t = 0$ fs, and dashed line: $t = 400$ fs. The dephasing time is 500 fs). (b) Optical absorption spectrum (with and without inhomogeneous broadening). (c) As in (a) but with a peak field energy of $4E_0$. (d) As in (b) but with a peak field energy of $4E_0$.

field strengths substantial oscillations appear above the band gap. The Sommerfeld factor and field-induced tunneling significantly affect the continuum portion of the absorption spectrum and continue to remove the well known divergence problem associated with the 1D DOS at all field strengths that we employ. For very large fields, tunneling-induced transparency occurs at certain spectral frequencies. Additionally, the influence of multiple subbands and inhomogeneous broadening was investigated.

This work was supported by National Science Foundation Grant No. DMR9705403 and by the Office of Naval Research. We are grateful to P. L. Knight for useful discussions.

[1] R. J. Elliott and R. Loudon, J. Phys. Chem. Solids **8**, 382 (1959); **15**, 196 (1969).
[2] T. Ogawa and T. Takagahara, Phys. Rev. B **44**, 8138 (1991).
[3] W. Franz, Z. Naturforsch. Teil A **13**, 484 (1958); L. V. Keldysh, Sov. Phys. JETP **34**, 788 (1958).
[4] S. Schmitt-Rink *et al.,* Adv. Phys. **38**, 89 (1989).
[5] S. Benner and H. Haug, Phys. Rev. B **47**, 15 750 (1993).
[6] U. Schwengelbeck and F. H. M. Faisal, Phys. Rev. A **50**, 632 (1994).
[7] See, for example, R. Rinaldi *et al.,* Phys. Rev. Lett. **73**, 2899 (1994); C. Constantin *et al.,* Phys. Rev. B **59**, R7809 (1999); K. H. Wang *et al.,* Phys. Rev. B **53**, R10 505 (1996); W. R. Tribe *et al.,* Appl. Phys. Lett. **73**, 3420 (1998).
[8] See, for example, F. Tassone and C. Piermarocchi, Phys. Rev. Lett. **82**, 843 (1999); F. Rossi *et al.,* Phys. Rev. Lett. **78**, 3527 (1997); S. Das Sarma and E. H. Hwang, Phys. Rev. B **54**, 1936 (1996); O. Mauritz *et al.,* Phys. Rev. Lett. **82**, 847 (1999).
[9] D. B. Tran Thoai and H. Thien Cao, Solid State Commun. **111**, 67 (1999).
[10] See, for example, J. Wang *et al.,* Appl. Phys. Lett. **69**, 287 (1996); G. Lehr *et al.,* Appl. Phys. Lett. **68**, 2327 (1996); S. Tiwari and J. M. Woodall, Appl. Phys. Lett. **64**, 2211 (1994).
[11] R. Grobe and J. H. Eberly, Phys. Rev. A **48**, 4664 (1993).
[12] M. Protopapas *et al.,* Phys. Rev. Lett. **79**, 4550 (1997).
[13] See H. Haug and S. W. Koch, *Quantum Theory of the Optical and Electronic Properties of Semiconductors* (World Scientific, Singapore, 1994), 3rd ed., and references therein.
[14] R. Zimmermann, *Spectroscopy and Dynamics of Collective Excitations in Solids,* edited by B. Di Bartoli (Plenum Press, New York, 1997), p. 126.
[15] Approximately 2 minutes CPU time on a 500 MHz DIGITAL Unix workstation is required to propagate 16 ps.
[16] F. Rossi and E. Molinari, Phys. Rev. B **53**, 16 462 (1996).
[17] J.-H. Son *et al.,* J. Opt. Soc. Am. B **11**, 2519–2527 (1994).
[18] A. Leitenstorfer *et al.,* Phys. Rev. Lett. **82**, 5140 (1999).
[19] S. Hughes and D. S. Citrin, Phys. Rev. B **59**, R5288 (1999); D. S. Citrin and S. Hughes, *ibid.* **60**, 13 272 (1999).